Sustainable Chemistry and Pharmacy 46 (2025) 102060

Contents lists available at ScienceDirect

Sustainable Chemistry and Pharmacy

journal homepage: www.elsevier.com/locate/scp

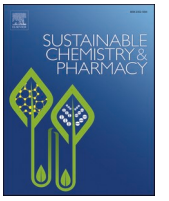

Holistic green synthesis at room temperature of MIL-53(Al) from aluminum slag and application for glucose conversion to 5-hydroxymethylfurfural

Guillermo Górtazar [a,b,1], Darío Fernández-González [b,1], Carmen Montoro [c,d], Jorge F. Romero [b], Anton Dafinov [e], Alejandro Jiménez [b], Ignacio Jiménez-Morales [b], Adrián Bogeat-Barroso [b], Félix Zamora [c,f], Mayra G. Álvarez [b,*], Elena López-Maya [b,**]

[a] Advanced Porous Materials Unit, IMDEA Energy Institute, Avda. Ramón de la Sagra 3, Móstoles, 28935, Madrid, Spain
[b] Department of Inorganic Chemistry, University of Salamanca, GIR-QUESCAT Group, Pl. Caídos, s/n, 37008, Salamanca, Spain
[c] Department of Inorganic Chemistry, Autonomous University of Madrid, 28049, Madrid, Spain
[d] Institute for Advanced Research in Chemical Sciences (IAdChem), Autonomous University of Madrid, 28049, Madrid, Spain
[e] Chemical Engineering Department, Rovira i Virgili University, Av Paisos Catalans 26, Tarragona, 43007, Spain
[f] Condensed Matter Physics Center (IFIMAC), Autonomous University of Madrid, 28049, Madrid, Spain

ARTICLE INFO

Handling Editor: Fabio Aricò

ABSTRACT

Herein, we report the first example of MOF synthesis employing aluminum slags as a waste resource. This synthesis was exclusively carried out from waste materials, under ambient conditions in water, thus aligning with the guiding principles of Green Chemistry. The resulting MIL-53(Al) material was further functionalized with SnO_2 nanoparticles and tested as catalyst for the dehydration of glucose to 5-hydroxymethylfurfural (5-HMF), showing a tenfold increase in catalytic efficiency compared to unsupported SnO_2.

1. Introduction

Metal-organic frameworks (MOFs) have emerged as a relevant class of crystalline materials, characterized by their high porosity and exceptional tunable degree for both organic and inorganic structural components. These features make MOFs fascinating materials for several applications in a variety of fields, such as gas storage, catalysis, biomedical imaging, etc (Zhou et al., 2012). Among the various categories of MOFs, MIL-53(Al) stands out as one of the most well-known materials due to its unique properties. MIL-53(Al) exhibits excellent chemical and thermal stability and presents a "breathing" behavior during adsorption processes (Férey et al., 2003). Despite its numerous attractive properties, traditional MIL-53 synthesis based on solvothermal methods requires high energy consumption, which is a significant drawback. Consequently, in the last few years, efforts have been made to develop new preparation methods under environmentally and economically favorable conditions or using different low-cost precursors. In this regard,

* Corresponding author.
** Corresponding author.
E-mail addresses: mgalvarez@usal.es (M.G. Álvarez), elenalopez@usal.es (E. López-Maya).
[1] These authors contributed equally to this work.

https://doi.org/10.1016/j.scp.2025.102060
Received 4 March 2025; Received in revised form 13 May 2025; Accepted 26 May 2025
Available online 30 May 2025

Sánchez-Sánchez et al. successfully synthesized prominent MOFs, like MIL-53(Al), MOF-74, and IRMOF-1, at room temperature from commercially available precursors using water as solvent (Sánchez-Sánchez et al., 2015). In addition, utilizing waste resources can significantly reduce production costs. In this sense, different authors have recently reported the use of waste materials for MOFs synthesis. For example, polyethylene terephthalate (PET) bottles have been used as a source of the terephthalic acid (H_2BDC) linker to synthesize several MOFs (Manju et al., 2013; Deleu et al., 2016), and various research groups have investigated the feasibility of metal recovery for high-value-added MOFs synthesis (Zhan et al., 2018; Kabtamu et al., 2020). Moreover, up to date, only a few articles have reported the simultaneous use of both types of solid wastes (i.e., linker and metals) as reagent sources (Zhang et al., 2020; Crickmore et al., 2021). Specifically, MIL-53(Al) material has been synthesized from PET bottles and different waste metal materials, such as aluminum beverage cans (Farajmand et al., 2020), aluminum foil (Panda et al., 2020) or Li-ion batteries (Lagae-Capelle et al., 2020). In these MIL-53(Al) synthesis approaches, dimethylformamide (DMF) was chosen as solvent and employed moderate or high reaction temperature conditions. Therefore, to fully fulfill the requirements of a circular economy approach, it is essential to develop a complete synthesis process based on waste sources for both the metal centers and the organic linker, search for a greener solvent and decrease the reaction temperature conditions.

On the other hand, one of the most dangerous and abundant metal waste products is salt cake, also known as saline slag, a by-product resulting from the aluminum recycling process. In Europe, it is classified as a hazardous waste because of its high toxicity and harmful effects on both the environment and living organism (Panda et al., 2020). The valorization of this waste can be accomplished after being subjected to physicochemical processes that recover a fraction of its aluminum content (Jiménez et al., 2022). In this context, numerous studies have explored the use of salt cake as an aluminum source for preparing high-value-added materials, like alumina (Das et al., 2007), zeolites (Yoldi et al., 2019), and layered double hydroxides (LDHs) (Santamaría et al., 2020). To the best of our knowledge, this novel environmentally friendly pathway has not yet been reported for the preparation of aluminum-based MOFs.

In the current work, we report for the very first time the successful and sustainable synthesis of MIL-53(Al) by exclusively using waste resources, specifically bottle-derived PET and aluminum slag, as MOF precursors through a simple pathway at room temperature in water, thus aligning with the Green Chemistry principles. The resulting MOF, designated as MIL-53-W, exhibited physical and chemical properties closely matching those of MIL-53(Al) prepared from commercial chemical reagents, denoted as MIL-53-C. Furthermore, we also evaluated the performance of the MIL-53-W system in key MOFs applications, particularly as a support for active nanoparticles typically used in heterogeneous catalysis.

2. Experimental

2.1. Chemicals

Saline slags were kindly supplied by IDALSA (Ibérica de Aleaciones Ligeras S.L., Spain). Terephthalic acid or 1,3-benzenedicarboxylic acid (H_2BDC, 99 %) and tin(IV) chloride pentahydrate ($SnCl_4{\cdot}5H_2O$, 98 %) were purchased from Merck. Aluminum nitrate nonahydrate ($Al(NO_3)_3{\cdot}9H_2O$, 98 %), ethylene glycol, and glucose were purchased from Scharlab. All reagents and solvents were used as received without any previous purification.

2.2. Materials preparation

2.2.1. Preparation of MIL-53-C

MIL-53-C was prepared by following the methodology previously reported elsewhere (Sánchez-Sánchez et al., 2015). Typically, 6.6 g (40 mmol) of H_2BDC was dissolved in 58 mL of water containing 3.2 g (80 mmol) of NaOH. This solution was added dropwise into another clear solution formed by dissolving 30 g (80 mmol) of $Al(NO_3)_3{\cdot}9H_2O$ salt under mechanical stirring. The mixture was maintained under stirring at room temperature for one week. The obtained white precipitate was washed with distilled water repeatedly and dried at 50 °C overnight. Yield = 82 %.

2.2.2. Preparation of MIL-53-W

Following the same methodology as for the synthesis of MIL-53-C, 8.5 mmol of H_2BDC extracted from PET by simple basic hydrolysis (Singh et al., 2018) (see Supporting Information) were dissolved in an aqueous solution (6 mL) containing 19 mmol of NaOH. This solution was added dropwise over 25 mL of the aluminum extraction solution (see Supporting Information). The content of aluminum was determined by inductively coupled plasma-optical emission spectroscopy, ICP-OES (9.3 g/L). Yield = 78 %.

2.2.3. Preparation of MIL-53@SnO_2 composites

The MIL-53@SnO_2 composites were synthesized with two different SnO_2 NPs loadings (10 wt% and 20 wt%, referred to as MIL-53@SnO_2-10 and MIL-53@SnO_2-20, respectively), by the bottle-around-ship methodology. An aqueous solution of Na_2BDC (8.5 mmol of H_2BDC and 19 mmol of NaOH) was prepared separately and added dropwise to 25 mL of the acidic slag aluminum solution, in which 100 mg or 200 mg of SnO_2 nanoparticles have been previously dispersed using ultrasonication, giving rise to MIL-53@SnO_2-10 and MIL-53@SnO_2-20, respectively (see Supporting Information for the preparation of SnO_2 nanoparticles). ICP-OES (Al: 4.4 ppm, Sn: 2.9 ppm; Al: 4.8 ppm, Sn: 6.7 ppm, respectively). Yield = 73 % and 66 %, respectively.

2.3. Characterization techniques

Thermogravimetric analyses (TGA) were performed on a SDT Q600 equipment, using a reactive air atmosphere and at a heating rate of 10 K/min up to 1073 K. Powder X-ray diffraction (PXRD) patterns were registered on a Bruker D8 Advance Eco diffractometer. N_2 adsorption isotherms were measured at 77 K on a Micromeritics 3Flex advanced gas adsorption instrument. Pore size distributions were obtained from the adsorption branch of the isotherms using the DFT (Density Functional Theory) method. Prior to starting the measurements, powder samples were heated overnight at 423 K and outgassed to 10^{-1} Pa. Fourier Transform Infrared (FT-IR) spectra were acquired with a Pike single-reflection ATR diamond/ZnSe accessory in a JASCO FT/IR-4700 spectrophotometer. Approximately 1 mg of samples were used to perform the analyses. Raman spectroscopy measurements were performed at room temperature using a LabRAM HR Evolution micro-Raman spectrometer (Horiba Jobin Yvon), equipped with a solid-state laser operating at a wavelength of 785 nm and a 100 × objective lens, yielding a laser spot size of approximately 1 μm^2. A JEOL F200 TEM ColdFEG operated at 200 kV was used for the transmission electron microscopy characterization (TEM). STEM images were recorded from the JEOL bright-field (BF) and high-angle annular dark-field (HAADF) detectors with a camera length of 150 mm. The samples were prepared by dispersing the as-prepared catalysts in ethanol and then drop casting the suspension on a standard 3 mm holey copper grid and letting the ethanol evaporate at room temperature. STEM-EDS mapping was recorded from an EDS Centurio detector (silicon drift) with an effective area of 100 mm^2 and 133 eV of energy resolution. Scanning electron microscopy (SEM) images were collected with an Electron Beam Lithography eLINE-PLUS de Raith GmbH with a resolution of 1 nm. The samples were previously coated with Cr. Inductively coupled plasma-optical emission spectroscopy analyses were performed in a PERKIN-ELMER OPTIMA 8300 spectrometer.

2.4. Catalytic tests

The conversion of glucose to 5-hydroxymethylfurfural (5-HMF) was carried out following the procedures reported by Jiménez-Morales et al., 2014, 2015. In these studies, the authors demonstrated that biphasic systems such as methyl isobutyl ketone (MIBK)/water improve the overall efficiency of HMF extraction by facilitating the partitioning of HMF into the organic phase. Briefly, the catalytic reaction was performed in an Ace pressure tube of 10 mL provided with a screw top of Teflon, at 453 K and 100 min of reaction time. Zero time was recorded when the temperature reached 453 K; the stirring rate was 400 rpm. The reaction was carried out with 30 mg of catalyst, 85 mg of glucose in 0.78 mL of H_2O and 2.1 mL of MIBK. The liquid phases were separated and filtered by

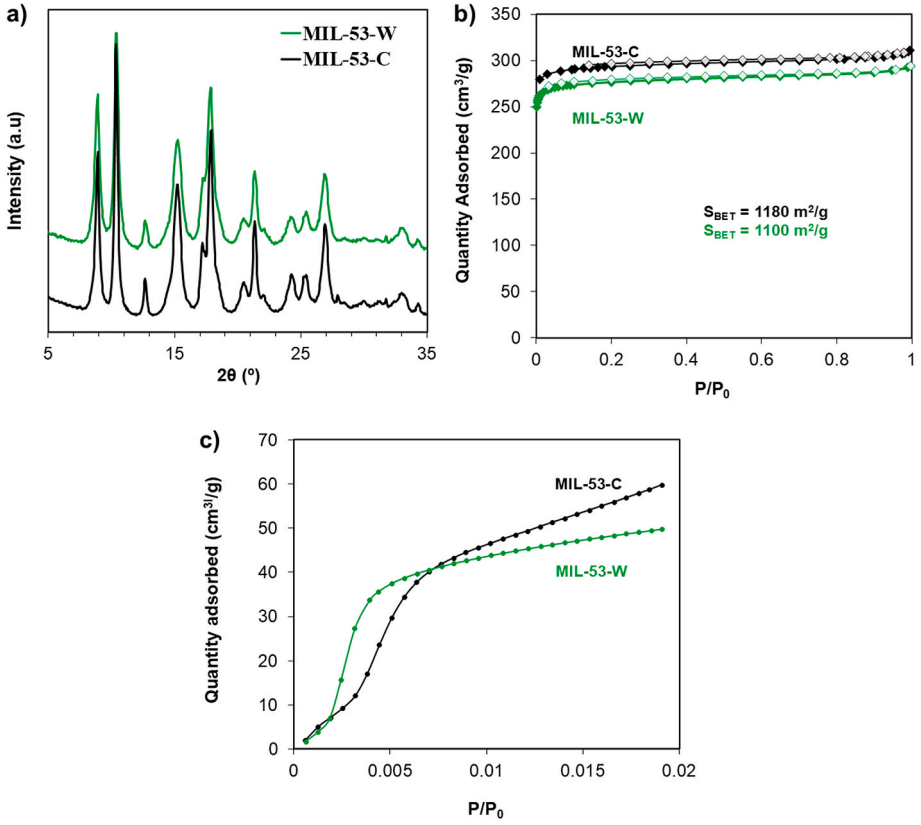

Fig. 1. a) PXRD patterns of MIL-53-W and MIL-53-C; b) N_2 adsorption isotherms at 77 K of MIL-53-W and MIL-53-C; c) CO_2 adsorption isotherms at 298 K of MIL-53-W and MIL-53-C.

0.45 μm nylon filter membrane. Glucose and fructose products were separated by an Agilent 1200 high performance liquid chromatography (HPLC) system equipped with a quaternary pump, autosampler, refractive index detector, and a Rezek ROA column oven. The mobile phase was 0.01 M H_2SO_4 with a flow rate of 0.6 mL min^{-1}. The 5-HMF was analyzed in both organic and aqueous phases, and it was determined using an Agilent 7890A gas chromatography equipment coupled to an MS220 ion trap mass spectrometer. Glucose conversion, HMF selectivity and yield were calculated according to the following equations:

$$\text{Glucose conversion(mol\%)} = \frac{(\textbf{\textit{mol of starting glucose}} - \textbf{\textit{mol of remaining glucose}})\ \textbf{\textit{x}}\ \mathbf{100}}{\textbf{\textit{mol of starting glucose}}}$$

$$5 - \textit{HMF selectivity}\ (\textit{mol\%}) = \frac{\textbf{\textit{Moles of produced}}\ \mathbf{5} - \textbf{\textit{HMF x}}\ \mathbf{100}}{\textbf{\textit{Moles of glucose reacted}}}$$

$$5 - \text{HMF yield}\ (\%) = \frac{\textbf{\textit{Conversion x Selectivity}}}{\mathbf{100}}$$

3. Results and discussion

Different characterization techniques confirmed the success of this green synthesis approach. The powder X-ray diffraction (PXRD) pattern of MIL-53-W matches well with that of MIL-53-C, with the most prominent characteristic reflection peaks consistently appearing at the corresponding diffraction angles (Fig. 1a). The main diffraction peaks at 9° and 10.5° are assigned to (101) and (200) crystallographic planes, respectively (Jin et al., 2022; Xiao et al., 2019; Loiseau et al., 2004). Thermogravimetric analysis (TGA) results demonstrate that both MIL-53 materials exhibit similar thermal stability, starting to decompose above *ca.* 790 K, with the observed mass loss corresponding to the combustion of the organic linker (Fig. S3). It is noteworthy that both MOFs exhibit a lower mass loss attributable to H_2BDC (14 wt%) as compared to the value of 30 wt% reported for conventional MIL-53 materials synthesized by the solvothermal methodology (Loiseau et al., 2004). However, the mass loss found for both MIL-53 materials presented here is in good agreement with previous studies where MIL-53 was also prepared at room temperature (Sánchez-Sánchez et al., 2015). Chemical functional groups of both materials were examined by Fourier-transform infrared (FT-IR) and Raman (FT-Raman) spectroscopy. Fig. S4 shows the FT-IR spectra of the MIL-53-W and MIL-53-C samples, where the significant bands are typically turned up at similar wavenumbers. Thus, the absorption band centered at 1416 cm^{-1} with a shoulder at 1440 cm^{-1} is ascribed to carboxylate (COO^-) symmetric stretching vibrations, while the band appearing at 1608 cm^{-1} is attributed to the asymmetric stretching mode. The bands at 738 cm^{-1} and 1510 cm^{-1} correspond to the vibrations of the phenyl ring in the organic linker. An additional band located at 1701 cm^{-1} is attributed to the carboxylic (-COOH) group, due to the presence of free terephthalic acid in the porous structure of the solids (Mounfield and Walton, 2015). In addition, Fig. S5 shows the TF-Raman spectra of both samples, whose profiles are fairly similar. The most prominent vibrational spectra appear in the wavenumber range of 1590–1630 cm^{-1} and are attributed to the asymmetric stretching vibration modes of the COO^- groups from the organic linkers coordinated to the framework. The corresponding symmetric stretching vibration modes are observed in the frequency range of 1460–1490 cm^{-1}. The vibrational band observed between 860 and 890 cm^{-1} is assigned to the bending vibrations of the aromatic ring and a vibrational mode appearing in the range of 1140–1150 cm^{-1} is associated with the stretching of the carboxylate group and the aromatic ring (Rehman et al., 2024). This indicates that both as-synthesized MOF materials present related structures. In order to examine the permanent porosity of both MIL-53 materials, N_2 physical sorption experiments at 77 K were conducted, and the corresponding isotherms are presented in Fig. 1b. Both MOFs exhibit BET surface areas above 1000 m^2/g, consistent with the values found in the literature (Sánchez-Sánchez et al., 2015; Loiseau et al., 2004), as well as similar narrow pore size distributions (Fig. S7), with a maximum at 1 nm and 1.1 nm, for MIL-53-W and MIL-53-C, respectively, which corresponds well with the MIL-53(Al) structure, which presents a channel diameter of about 10 Å (Li et al., 2023; Vanduyfhuys et al., 2012). Besides, the morphology of both samples is indistinguishable, as seen by TEM analysis (Fig. S6). In summary, this set of characterization studies performed on MIL-53-C and MIL-53-W revealed their structural similarity, thereby confirming that pure MIL-53 can be successfully synthesized from aluminum slag and PET bottles at room temperature. Furthermore, CO_2 sorption isotherms at 298 K have also been registered for the MIL-53-W and MIL-53-C systems, since MIL-53(Al) has been widely studied as an adsorbent for CO_2 gas separation due to its strong interactions with this molecule (Heymans et al., 2012; Finsy et al., 2009; Bourrelly et al., 2005). As shown in Fig. 1c, the CO_2 uptake at 298 K is 49.9 cm^3/g for MIL-53-W and 59.9 cm^3/g for MIL-53-C, both being well in agreement with the reported value of 56.5 cm^3/g (Rallapalli et al., 2011), which suggests a comparable CO_2 interaction and adsorption capacity for both materials.

MOFs are excellent candidates as supports for nanoparticles (NPs) due to their stable and permanent porous structure. In recent years, numerous researchers have explored the incorporation of NPs into different MOFs. In this connection, using these porous materials as an encapsulating matrix offers significant advantages over conventional supported catalysts, particularly in terms of stability and catalytic selectivity (Yu et al., 2017; Li et al., 2018; Rivera-Torrente et al., 2018). As a proof of concept, the as-synthesized MIL-53-W material was employed as catalyst support for SnO_2 NPs, and the resulting hybrid material was tested in the 5-HMF production from glucose. Biomass-derived glucose is a key feedstock for producing green platform chemicals (Herbst and Janiak, 2016; An et al., 2021). Among these, 5-HMF stands out as a crucial intermediate for the synthesis of a wide variety of high value-added compounds, including, for instance, 2,5-furandicarboxylic acid (FDCA) (Zhang et al., 2023) and 2,5-bis(hydroxymethyl)furan (BHMF) (Vikanova et al., 2021). These molecules find applications in the development of sustainable polymers and functional materials, offering viable alternatives to conventional petrochemical-based monomers. The 5-HMF production from glucose involves a

two-step catalytic process: (i) isomerization of glucose to fructose mediated by a Lewis acid or base, and (ii) dehydration of fructose to 5-HMF by a Brønsted acid (Jiménez-Morales et al., 2014). The SnO_2 surface presents adsorbed water molecules that, upon dissociation, lead to hydroxyl (-OH) groups of acidic or basic nature depending on their coordination environment. It also displays uncoordinated tin and oxygen atoms, as well as defective sites (both metal and oxygen) that can act as protonated or aprotic acidic or basic sites (Deka et al., 2020). Therefore, SnO_2 is an excellent candidate as catalyst for 5-HMF production. In this sense, different forms of SnO_2 (NPs, amorphous oxide, mixture of oxides, etc.) have been studied as catalysts in the conversion of glucose to 5-HMF (Wang et al., 2021; Zhang et al., 2015; Liu et al., 2023). In addition, tin oxide is considered a green, non-toxic and cost-effective solid acid. Meanwhile, MIL-53(Al) modified with different functional groups (-NH_2, –NO_2 or –SO_3H), polyoxometalates or heterometallic MIL-53(Al–Sn) have also been investigated recently as catalysts for the 5-HMF production (Lara-Serrano et al., 2021; Z.Z et al., 2023; Chen et al., 2014; Yu et al., 2024). It is worth highlighting that the most promising results were obtained by using the mixed-metal MOF functionalized with –NO_2 groups, the so-called MIL-53(Al–Sn)–NO_2 material. This metal combination of Al^{3+} and Sn^{4+} has been tested in other materials, like Sn,Al-beta zeolites, also yielding good results for the glucose conversion to 5-HMF (An et al., 2021). In this context, MIL-53-W and SnO_2 NPs were combined to obtain a MIL-53@SnO_2 hybrid material, which was tested as catalyst in the conversion reaction of glucose into 5-HMF. MIL-53@SnO_2-10 and MIL-53@SnO_2-20 composites were characterized by PXRD, FT-IR spectroscopy, and N_2 physical adsorption. The original topology of the MIL-53 framework is retained after the incorporation of the SnO_2 NPs, as evidenced from their PXRD patterns (Fig. 2a). Besides, a decrease in the intensity of the diffraction peaks corresponding to MIL-53 is observed with increasing SnO_2 content, as a consequence of a lower relative amount of MIL-53 in the hybrid materials. Notably, no peaks ascribable to the SnO_2 phase were detected, suggesting a good distribution of small-sized SnO_2 NPs within the MOF framework despite the expected relatively high loading. N_2 adsorption isotherms at 77 K indicate that SnO_2 incorporation does not block the access to the porous network, although it is responsible for a significant decrease of the adsorption capacity, the total pore volume and thereby of the BET surface area (Fig. 2b and Table S1). Moreover, SnO_2 loading was simultaneously evaluated by the TGA and ICP-OES techniques, both yielding a SnO_2 content of approximately 9 wt% and 17 wt% for MIL-53@SnO_2-10 and MIL-53@SnO_2-20, respectively, very close to the nominal values.

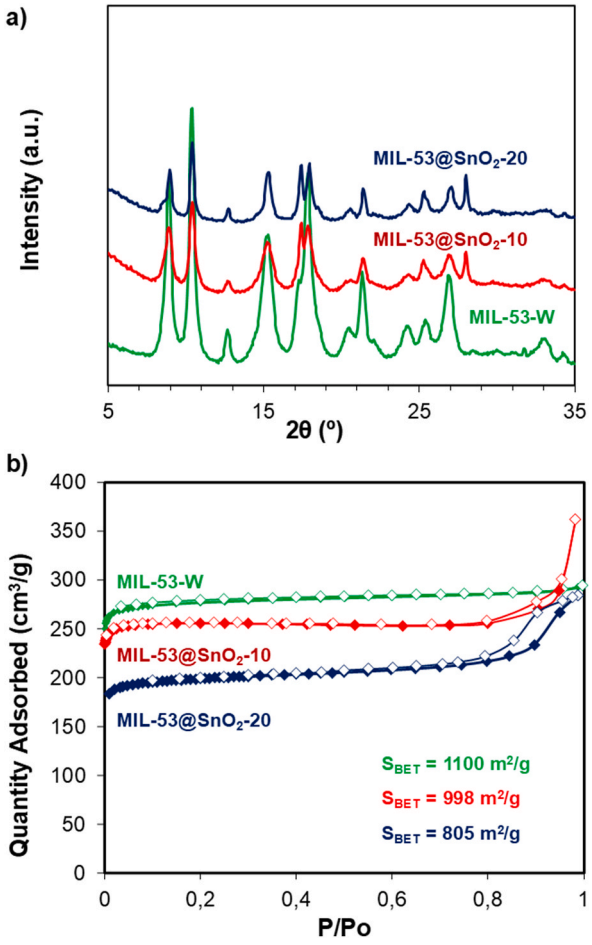

Fig. 2. a) PXRD patterns of MIL-53-W, MIL-53@SnO_2-10, and MIL-53@SnO_2-20; b) N_2 adsorption isotherms at 77 K of MIL-53-W, MIL-53@SnO_2-10, and MIL-53@SnO_2-20.

The one-pot conversion of glucose to 5-HMF was performed in a biphasic water/methyl-isobutyl ketone system at 453 K for 100 min. Table 1 lists the results obtained with the pristine MIL-53, unsupported SnO_2 NPs, and MIL-53@SnO_2 composites. Both MIL-53-W and MIL-53-C show negligible 5-HMF yield (*ca.* 2 %), thus indicating their inertness as mere supports and evidencing their similar chemical behavior. Glucose conversion resulted lower than expected in both synthesized MIL-53, despite the known characteristics of Lewis acids (Table S2). This can be attributed to the competition of H_2O molecules, which is the solvent selected for this reaction, for the available Lewis acid sites of MIL-53. Then, the protic character of our chosen solvent generates Brønsted acid sites, consequently the conversion of glucose is prevented. This effect has been recently reported by Lara-Serrano et al. (2021). In stark contrast, the unsupported SnO_2 NPs are catalytically active in this reaction, yielding 21 % conversion of glucose to 5-HMF (Table 1). The SnO_2 NPs boosted the glucose conversion to nearly 100 % (Table S2), which can be attributed to a certain Lewis acid character of the oxide and the ability of Sn to coordinate the carbonyl group of the open form of glucose (Moliner et al., 2010). Then, dehydration is overcome to form 5-HMF. It must be underlined that the synthesized SnO_2 NPs have been formed by pH adjustment in ethylene glycol (see Supporting Information for further details) and no subsequent thermal treatments were applied upon drying. This fact, together with the aqueous medium of reaction, makes it possible to expect the presence of Brønsted acid sites, which are able to form 5-HMF by a dehydration pathway. Thermogravimetric analysis of SnO_2 NPs is consistent with this hypothesis (Fig. S1a), showing a weight loss of 11.3 % at about 373 K corresponding to physisorbed water molecules, followed by a second weight loss of 10.5 % at 566 K, which corresponds to dehydroxylation processes, thus confirming the presence of a considerable amount of hydroxyl groups on its structure. As previously mentioned, Brønsted acids are necessary to dehydrate fructose and convert it into 5-HMF. The catalytic results obtained suggest that although the synthesis method incorporates SnO_2 hydroxyl groups (Fig. S1), and thus it presents Lewis and Brønsted basic sites (Fig. S2), SnO_2 lacks the Brønsted acidity required to facilitate the conversion of fructose into 5-HMF. Zhao et al. noted that a Brønsted/Lewis acidity ratio far from unity promotes the formation of secondary products such as humins (Scheme S1), which may explain why higher yields were not achieved despite complete glucose conversion (Zhao et al., 2018). The formation of humins was indeed noted as a side product during the reaction. Fig. S15 displays the FT-IR spectrum of the solid humins recovered from the pressure glass tube after the reaction.

The MIL-53@SnO_2-10 and MIL-53@SnO_2-20 composites also exhibited high glucose conversion rates (Table S3), and the yields of 5-HMF obtained, approximately 17 % and 18 % respectively (Table 1), were comparable to those achieved using unsupported SnO_2 nanoparticles. However, taking into account the glucose conversion, MIL-53@SnO_2-10 catalyst seems to be more selective to 5-HMF.

In addition, it should be highlighted that the incorporation of SnO_2 NPs into the MIL-53 porous structure greatly increases the 5-HMF/SnO_2 ratio values (Table 1). Thus, supporting SnO_2 NPs within the MIL-53-W framework leads to a ten-fold increase in catalytic activity (in terms of 5-HMF yield). This enhanced catalytic activity of MIL-53-W-supported SnO_2 is attributed to the presence of well-dispersed nanoparticles, about 2 nm in size, throughout the MOF structure, as clearly shown in the corresponding TEM and STEM-HAADF micrographs (Figures S11, S12 and S13), and EDX chemical maps from SEM (Fig. S14). Control experiments performed with a physical mixture of MIL-53-W and SnO_2 NPs (10 wt%), labelled as MIL-53-W + SnO_2, further validated the synergistic effect between both components in the synthesized MIL-53@SnO_2 composites. The catalytic activity of this physical mixture is considerably lower as compared to the MIL-53@SnO_2-10 composite (see Table 1). In addition, the heterogeneous nature of MIL-53@SnO_2-10 allows to reuse this material, showing small activity loss (less than 15 %) achieving a yield to 5-HMF of 14 % after three reaction cycles.

Neither levulinic acid (LA) nor formic acid (FA) were observed in any of the tests performed regardless of the SnO_2 loading. This indicates that humins and 5-HMF are the main compounds produced, probably due to an insufficient content of Brønsted acid sites, as mentioned above. In this context, Shen et al. reported that a signal at approximately 1710 cm^{-1} in the IR spectrum can be attributed to a carbonyl group conjugated with a C═C bond, resulting from the aldol condensation between 5-HMF and LA (Shen et al., 2020). The very low intensity found for this band in the FT-IR of the recovered humin may indicate negligible condensation between 5-HMF and LA, in accordance with our analysis, where LA has not been detected. Hence, tentatively, humins can be mostly formed by etherification of HMF units, Lewis acidity playing a role in promoting the initial steps of 5-HMF dehydration and subsequent reactions leading to humin formation with residual reactions with other possible molecules (Shen et al., 2020).

In addition, small variations in temperature have shown a great effect on the catalytic performance of the MIL-53@SnO_2 material. As expected, decreasing the temperature, catalyst amount and reaction time leads to a reduced yield of 5-HMF, while a small increase in the temperature seems to slightly favor the formation of 5-HMF from ca. 17 % to ca. 19 % at 453 K and 463 K, respectively (Table S4). Interestingly, excessive increments in either reaction time or catalyst amount result in a slight decrease in 5-HMF yield. This may be attributed to the formation of humins under these conditions, which are known to compete with 5-HMF formation and lower the overall selectivity of the process.

Table 1
Conversion of glucose to 5-HMF. Reaction conditions: temperature = 453 K, reaction time = 100 min.

Catalyst	SnO_2 content (wt.%)	5-HMF/SnO_2 (mol/mol)	Yield (%)
MIL-53-C	–	–	2
MIL-53-W	–	–	2
SnO_2 NPs	100	0.5	21
MIL-53@SnO_2-10	9	4.5	17
MIL-53@SnO_2-10[a]	9	3.5	14
MIL-53@SnO_2-20	17	2.7	18
MIL-53+SnO_2	10	0.5	2

[a] Recycled experiment: 3rd cycle.

The structural, morphological and textural properties of the used catalyst were also evaluated. The used MIL-53@SnO_2-10 presents a morphology rather similar to its fresh counterpart (Fig. S19). The SnO_2 NPs still remain in the support after several reuses and no significant differences were observed in their population density, although it is possible that SnO_2 NPs undergo certain agglomeration. In addition, ICP analysis confirms that the Sn/Al atomic ratios in the fresh (0.151) and used (0.130) catalysts remain nearly unchanged, which highlights the stability of this material as a catalytic system even at high temperatures of reaction (Table S5). The structure of the used catalyst remains; however, PXRD analysis (Fig. S16) shows a clear decrease in crystallinity after the catalytic cycles. Furthermore, BET measurements (Fig. S18) indicate an approximate 80 % reduction in surface area in the used material. This significant decrease is likely due to pore blockage by humins formed during the reaction (as indicates the white-to-brownish color change in the catalyst, Fig. S20), which can limit the accessibility of reactants to the active sites, thus reducing the catalytic performance in successive cycles.

4. Conclusions

In this work, we have attempted to approach a zero-waste concept through the integral synthesis of a MOF material with multiple potential applications. For the first time, the MIL-53 material has been synthesized by valorizing aluminum slag and PET bottles as precursors for the metal and ligand building blocks, respectively. In addition, the whole synthesis was performed at room temperature using water as a solvent exclusively in a holistic green chemistry approach. The obtained MIL-53-W material presented physicochemical properties equivalent to those shown by its counterpart prepared from commercial precursors and, at the same time, comparable to a MIL-53(Al) material prepared by solvothermal methods and using organic solvents, thus indicating the viability of the proposed method.

We have further explored the potential application of MIL-53-W as catalyst support of SnO_2 NPs for biomass transformations, specifically the one-pot conversion of glucose to 5-HMF. The resulting MIL-53@SnO_2 composites provided normalized yields up to ten-fold higher than the unsupported SnO_2 NPs, and the catalyst could be reused without significant loss in glucose conversion and 5-HMF yield, and the material preserved its structure and morphology after catalysis highlighting the stability of this material as a catalytic system, even at moderate-high reaction temperatures and liquid/aqueous media. This study may pave the way for sustainability goals and circular economy in materials engineering.

CRediT authorship contribution statement

Guillermo Górtazar: Methodology, Investigation. **Darío Fernández-González:** Methodology, Investigation. **Carmen Montoro:** Writing – review & editing, Methodology, Investigation. **Jorge F. Romero:** Methodology, Investigation. **Anton Dafinov:** Investigation, Writing – review & editing. **Alejandro Jiménez:** Methodology, Investigation. **Ignacio Jiménez-Morales:** Writing – review & editing, Methodology, Investigation, Funding acquisition. **Adrián Bogeat-Barroso:** Writing – review & editing, Methodology, Investigation. **Félix Zamora:** Writing – review & editing, Methodology, Investigation, Funding acquisition. **Mayra G. Álvarez:** Writing – review & editing, Writing – original draft, Supervision, Methodology, Investigation, Funding acquisition, Formal analysis, Data curation, Conceptualization. **Elena López-Maya:** Writing – review & editing, Writing – original draft, Supervision, Methodology, Investigation, Formal analysis, Data curation, Conceptualization.

Funding sources

Authors acknowledge funding from the Research Program I, C2 call of the University of Salamanca (PIC2-2022-08). I.J.M acknowledges Research Program I, C1 call of the University of Salamanca (PIC1-2023-07). F. Z. acknowledges financial support from the Spanish Ministry of Science and Innovation, through the PID2022-138908NB-C31 and Universities through the “María de Maeztu” Programme for Units of Excellence in R&D CEX2023-001316-M.

Declaration of competing interest

The authors declare that they have no known competing financial interests or personal relationships that could have appeared to influence the work reported in this paper.

Acknowledgements

The authors would like to thank S. Plana Ruiz, F. J. Carmona Fernández, and M. A. Palacios for their support in the characterization of the samples.

Appendix B. Supplementary data

Supplementary data to this article can be found online at https://doi.org/10.1016/j.scp.2025.102060.

Data availability

Data will be made available on request.

References

An, H., Kweon, S., Kang, D.C., Shin, C.H., Kim, J.F., Park, M.B., Min, H.K., 2021. Cascade conversion of glucose to 5-hydroxymethylfurfural over Brönsted-Lewis bi-acidic SnAl-beta zeolites. Kor. J. Chem. Eng. 38, 1161–1169. https://doi.org/10.1007/s11814-021-0752-1.

Bourrelly, S., Llewellyn, P.L., Serre, C., Millange, F., Loiseau, T., Férey, G., 2005. Different adsorption behaviors of methane and carbon dioxide in the isotypic nanoporous metal terephthalates MIL-53 and MIL-47. J. Am. Chem. Soc. 127, 13519–13521. https://doi.org/10.1021/ja054668v.

Chen, J., Li, K., Chen, L., Liu, R., Huang, X., Ye, D., 2014. Conversion of fructose into 5-hydroxymethylfurfural catalyzed by recyclable sulfonic acid-functionalized metal-organic frameworks. Green Chem. 16, 2490–2499. https://doi.org/10.1039/c3gc42414f.

Crickmore, T.S., Sana, H.B., Mitchell, H., Clark, M., Bradshaw, D., 2021. Toward sustainable syntheses of Ca-based MOFs. Chem. Commun. 57, 10592–10595. https://doi.org/10.1039/d1cc04032d.

Das, B.R., Dash, B., Tripathy, B.C., Bhattacharya, I.N., Das, S.C., 2007. Production of η-alumina from waste aluminium dross. Miner. Eng. 20, 252–258. https://doi.org/10.1016/j.mineng.2006.09.002.

Deka, R.C., Deka, A., Deka, P., Saikia, S., Baruah, J., Sarma, P.J., 2020. Recent advances in nanoarchitectonics of SnO 2 clusters and their applications in catalysis. J. Nanosci. Nanotechnol. 20, 5153–5161. https://doi.org/10.1166/jnn.2020.18539.

Deleu, W.P.R., Stassen, I., Jonckheere, D., Ameloot, R., De Vos, D.E., 2016. Waste PET (bottles) as a resource or substrate for MOF synthesis. J. Mater. Chem. A 4, 9519–9525. https://doi.org/10.1039/c6ta02381a.

Farajmand, B., Dalali, N., Keshavarz, S., Lakmehsari, M.S., 2020. Application of MIL-53(Al) prepared from waste materials for solid-phase microextraction of propranolol followed by corona discharge-ion mobility spectrometry (CD-IMS). J. Pharm. Biomed. Anal. 189, 113418. https://doi.org/10.1016/j.jpba.2020.113418.

Férey, G., Latroche, M., Serre, C., Millange, F., Loiseau, T., Percheron-Guégan, A., 2003. Hydrogen adsorption in the nanoporous metal-benzenedicarboxylate M(OH)(O2C-C6H4-CO2)(M = Al3+, Cr3+), MIL-53. Chem. Commun. 3, 2976–2977. https://doi.org/10.1039/b308903g.

Finsy, V., Ma, L., Alaerts, L., De Vos, D.E., Baron, G.V., Denayer, J.F.M., 2009. Separation of CO2/CH4 mixtures with the MIL-53(Al) metal-organic framework. Microporous Mesoporous Mater. 120, 221–227. https://doi.org/10.1016/j.micromeso.2008.11.007.

Herbst, A., Janiak, C., 2016. Selective glucose conversion to 5-hydroxymethylfurfural (5-HMF) instead of levulinic acid with MIL-101Cr MOF-derivatives. New J. Chem. 40, 7958–7967. https://doi.org/10.1039/c6nj01399f.

Heymans, N., Vaesen, S., De Weireld, G., 2012. A complete procedure for acidic gas separation by adsorption on MIL-53 (Al). Microporous Mesoporous Mater. 154, 93–99. https://doi.org/10.1016/j.micromeso.2011.10.020.

Jiménez, A., Rives, V., Vicente, M.A., Gil, A., 2022. A comparative study of acid and alkaline aluminum extraction valorization procedure for aluminum saline slags. J. Environ. Chem. Eng. 10, 1–10. https://doi.org/10.1016/j.jece.2022.107546.

Jiménez-Morales, I., Teckchandani-Ortiz, A., Santamaría-González, J., Maireles-Torres, P., Jiménez-López, A., et al., 2014. Selective dehydration of glucose to 5-hydroxymethylfurfural on acidic mesoporous tantalum phosphate. Appl. Catal. B Environ. 144, 22–28. https://doi.org/10.1016/j.apcatb.2013.07.002.

Jiménez-Morales, I., Moreno-Recio, M., Santamaría-González, J., Maireles-Torres, P., Jiménez-López, A., 2015. Production of 5-hydroxymethylfurfural from glucose using aluminium doped MCM-41 silica as acid catalyst. Appl. Catal. B Environ. 164, 70–76. https://doi.org/10.1016/j.apcatb.2014.09.002.

Jin, Z., Li, X., Li, T., Li, Y., 2022. Graphdiyne (CnH2 n-2)-based GDY/CuI/MIL-53(Al) S-scheme heterojunction for efficient hydrogen evolution. Langmuir 38, 15632–15641. https://doi.org/10.1021/acs.langmuir.2c02334.

Kabtamu, D.M., Wu, Y.N., Chen, Q., Zheng, L., Otake, K.I., Matović, L., Li, F., 2020. Facile upcycling of hazardous Cr-containing electroplating sludge into value-added metal-organic frameworks for efficient adsorptive desulfurization. ACS Sustain. Chem. Eng. 8, 11253–11262. https://doi.org/10.1021/acssuschemeng.0c03110.

Lagae-Capelle, E., Cognet, M., Madhavi, S., Carboni, M., Meyer, D., 2020. Combining organic and inorganic wastes to form metal-organic frameworks. Materials 13, 1–6. https://doi.org/10.3390/ma13020441.

Lara-Serrano, M., Morales-DelaRosa, S., Campos-Martin, J.M., Abdelkader-Fernández, V.K., Cunha-Silva, L., Balula, S.S., 2021. Isomerization of glucose to fructose catalyzed by metal-organic frameworks. Sustain. Energy Fuels 5, 3847–3857. https://doi.org/10.1039/d1se00771h.

Li, G., Zhao, S., Zhang, Y., Tang, Z., 2018. Metal–organic frameworks encapsulating active nanoparticles as emerging composites for catalysis: recent progress and perspectives. Adv. Mater. 30, 1–43. https://doi.org/10.1002/adma.201800702.

Li, X., Jiang, G., Jian, M., Zhao, C., Hou, J., Thornton, A.W., Zhang, X., Liu, J.Z., Freeman, B.D., Wang, H., Jiang, L., Zhang, H., 2023. Construction of angstrom-scale ion channels with versatile pore configurations and sizes by metal-organic frameworks. Nat. Commun. 14, 1–12. https://doi.org/10.1038/s41467-023-35970-x.

Liu, G., Liu, H., Zhang, J., Zhang, R., Zhang, H., Sun, Y., Peng, L., 2023. Efficient production of 5-hydroxymethylfurfural from concentrated carbohydrates and raw biomass over SnP2O7-SnO2 catalysts. ACS Sustain. Chem. Eng. 11, 18001–18010. https://doi.org/10.1021/acssuschemeng.3c05783.

Loiseau, T., Serre, C., Huguenard, C., Fink, G., Taulelle, F., Henry, M., Bataille, T., Férey, G., 2004. A rationale for the large breathing of the porous aluminum terephthalate (MIL-53) upon hydration. Chem. Eur J. 10, 1373–1382. https://doi.org/10.1002/chem.200305413.

Manju, P. Kumar Roy, Ramanan, A., Rajagopal, C., 2013. Post consumer PET waste as potential feedstock for metal organic frameworks. Mater. Lett. 106, 390–392. https://doi.org/10.1016/j.matlet.2013.05.058.

Moliner, M., Román-Leshkov, Y., Davis, M.E., 2010. Tin-containing zeolites are highly active catalysts for the isomerization of glucose in water. Proc. Natl. Acad. Sci. U. S. A. 107, 6164–6168. https://doi.org/10.1073/pnas.1002358107.

Mounfield, W.P., Walton, K.S., 2015. Effect of synthesis solvent on the breathing behavior of MIL-53(Al). J. Colloid Interface Sci. 447, 33–39. https://doi.org/10.1016/j.jcis.2015.01.027.

Panda, D., Patra, S., Awasthi, M.K., Singh, S.K., 2020. Lab cooked MOF for CO2Capture: a sustainable solution to waste management. J. Chem. Educ. 97, 1101–1108. https://doi.org/10.1021/acs.jchemed.9b00337.

Rallapalli, P., Prasanth, K.P., Patil, D., Somani, R.S., Jasra, R.V., Bajaj, H.C., 2011. Sorption studies of CO2, CH4, N2, CO, O2 and Ar on nanoporous aluminum terephthalate [MIL-53(Al)]. J. Porous Mater. 18, 205–210. https://doi.org/10.1007/s10934-010-9371-7.

Rehman, T.U., Agnello, S., Gelardi, F.M., Calvino, M.M., Buscarino, G., Cannas, M., 2024. Stimuli-responsive photoluminescent and structural properties of MIL-53 (Al) MOF for sensing applications. J. Phys. Condens. Matter 36. https://doi.org/10.1088/1361-648X/ad43a4.

Rivera-Torrente, M., Filez, M., Hardian, R., Reynolds, E., Seoane, B., Coulet, M.V., Oropeza Palacio, F.E., Hofmann, J.P., Fischer, R.A., Goodwin, A.L., Llewellyn, P.L., Weckhuysen, B.M., 2018. Metal-organic frameworks as catalyst supports: influence of lattice disorder on metal nanoparticle formation. Chem. Eur J. 24, 7498–7506. https://doi.org/10.1002/chem.201800694.

Sánchez-Sánchez, M., Getachew, N., Díaz, K., Díaz-García, M., Chebude, Y., Díaz, I., 2015. Synthesis of metal-organic frameworks in water at room temperature: salts as linker sources. Green Chem. 17, 1500–1509. https://doi.org/10.1039/c4gc01861c.

Santamaría, L., López-Aizpún, M., García-Padial, M., Vicente, M.A., Korili, S.A., Gil, A., 2020. Zn-Ti-Al layered double hydroxides synthesized from aluminum saline slag wastes as efficient drug adsorbents. Appl. Clay Sci. 187, 105486. https://doi.org/10.1016/j.clay.2020.105486.

Shen, H., Shan, H., Liu, L., 2020. Evolution process and controlled synthesis of humins with 5-hydroxymethylfurfural (HMF) as model molecule. ChemSusChem 13, 513–519. https://doi.org/10.1002/cssc.201902799.

Singh, S., Sharma, S., Umar, A., Mehta, S.K., Bhatti, M.S., Kansal, S.K., 2018. Recycling of waste poly(ethylene terephthalate) bottles by alkaline hydrolysis and recovery of pure nanospindle-shaped terephthalic acid. J. Nanosci. Nanotechnol. 18, 5804–5809. https://doi.org/10.1166/jnn.2018.15363.

Vanduyfhuys, L., Verstraelen, T., Vandichel, M., Waroquier, M., Van Speybroeck, V., 2012. Ab initio parametrized force field for the flexible metal-organic framework MIL-53(Al). J. Chem. Theor. Comput. 8, 3217–3231. https://doi.org/10.1021/ct300172m.

Vikanova, K., Redina, E., Kapustin, G., Chernova, M., Tkachenko, O., Nissenbaum, V., Kustov, L., 2021. Advanced room-temperature synthesis of 2,5-Bis(hydroxymethyl)furan-A monomer for biopolymers-from 5-hydroxymethylfurfural. ACS Sustain. Chem. Eng. 9, 1161–1171. https://doi.org/10.1021/acssuschemeng.0c06560.

Wang, K., Rezayan, A., Si, L., Zhang, Y., Nie, R., Lu, T., Wang, J., Xu, C., 2021. Highly efficient 5-hydroxymethylfurfural production from glucose over bifunctional SnOx/C catalyst. ACS Sustain. Chem. Eng. 9, 11351–11360. https://doi.org/10.1021/acssuschemeng.1c02870.

Xiao, H., Zhang, W., Yao, Q., Huang, L., Chen, L., Boury, B., Chen, Z., 2019. Zn-free MOFs like MIL-53(Al) and MIL-125(Ti) for the preparation of defect-rich, ultrafine ZnO nanosheets with high photocatalytic performance. Appl. Catal. B Environ. 244, 719–731. https://doi.org/10.1016/j.apcatb.2018.11.026.

Yoldi, M., Fuentes-Ordoñez, E.G., Korili, S.A., Gil, A., 2019. Zeolite synthesis from industrial wastes. Microporous Mesoporous Mater. 287, 183–191. https://doi.org/10.1016/j.micromeso.2019.06.009.

Yu, J., Mu, C., Yan, B., Qin, X., Shen, C., Xue, H., Pang, H., 2017. Nanoparticle/MOF composites: preparations and applications. Mater. Horiz. 4, 557–569. https://doi.org/10.1039/c6mh00586a.

Yu, M., Zhang, X.F., Yang, S., Bai, Y., Wang, Z., Yao, J., 2024. Defective MIL-53(Al)-NH2: a bifunctional Lewis-Brønsted acid catalyst for efficient 5-HMF production from glucose. J. Mol. Struct. 1307, 137976. https://doi.org/10.1016/j.molstruc.2024.137976.

Zhan, G., Ng, W.C., Lin, W.Y., Koh, S.N., Wang, C.H., 2018. Effective recovery of vanadium from oil refinery waste into vanadium-based metal-organic frameworks. Environ. Sci. Technol. 52, 3008–3015. https://doi.org/10.1021/acs.est.7b04989.

Zhang, M., Su, K., Song, H., Li, Z., Cheng, B., 2015. The excellent performance of amorphous Cr2O3, SnO2, SrO and graphene oxide-ferric oxide in glucose conversion into 5-HMF. Catal. Commun. 69, 76–80. https://doi.org/10.1016/j.catcom.2015.05.024.

Zhang, S., Jian, M., Zhang, Q., Xu, R., Qu, J., Luo, X., Li, X., Hu, J., Liu, R., Zhang, X., 2020. Recyclable printed circuit boards and alkali reduction wastewater: approach to a sustainable copper-based metal-organic framework. ACS Sustain. Chem. Eng. 8, 1371–1379. https://doi.org/10.1021/acssuschemeng.9b04754.

Zhang, Y., Cao, Y., Yan, C., Liu, W., Chen, Y., Guan, W., Wang, F., Liu, Y., Huo, P., 2023. Rationally designed Au-ZrOx interaction for boosting 5-hydroxymethylfurfural oxidation. Chem. Eng. J. 459, 141644. https://doi.org/10.1016/j.cej.2023.141644.

Zhao, Y., Wang, S., Lin, H., Chen, J., Xu, H., 2018. Influence of a Lewis acid and a Brønsted acid on the conversion of microcrystalline cellulose into 5-hydroxymethylfurfural in a single-phase reaction system of water and 1,2-dimethoxyethane. RSC Adv. 8, 7235–7242. https://doi.org/10.1039/c7ra13387a.

Zhou, H.C., Long, J.R., Yaghi, O.M., 2012. Introduction to metal − organic frameworks. Chem. Rev. 112, 673–674. https://doi.org/10.1021/cr300014x.

Z.Z., Zhang, L.L.Y., Chen, X., 2023. Applied Organom Chemis - 2023 - Zhang - Transformation of glucose to 5-hydroxymethylfurfural with Al and Sn mixed-metal.pdf. Appl. Organomet. Chem. 2. 38, e7310. https://doi.org/10.1002/aoc.7310.